J. Iron Steel Res. Int. (2019) 26:102–111
https://doi.org/10.1007/s42243-018-0215-z

ORIGINAL PAPER

Microstructural features and precipitation behavior of Ti, Nb and V microalloyed steel during isothermal processing

Qi Zhou[1] · Zhuang Li[2] · Zhan-shan Wei[2] · Di Wu[3] · Jin-yu Li[2] · Zhen-yao Shao[2]

Received: 30 August 2017 / Revised: 4 April 2018 / Accepted: 4 May 2018 / Published online: 7 January 2019

Abstract
Thermal simulations of Ti, Nb and V microalloyed steel were conducted using a thermomechanical simulator, and the microstructural evolution and the precipitation behavior during isothermal processing were analyzed. The results show that with increasing holding time, the microstructural constituents change from the martensite and bainitic ferrites to granular bainite and polygonal ferrite. The maximum hardness is obtained for the specimen after isothermal holding for 5 s due to the martensite strengthening effect. The hardness of the specimen decreases after isothermal holding for 10 s, because the strengthening contribution of fine dispersed precipitates becomes weaker. The hardness values of the specimens increase and then remain high after isothermal holding for 60 and 600 s. This is attributed to the contribution of the interphase precipitation hardening to the hardness of the studied steel. The precipitates in the specimen are coarsened after isothermal holding for 3600 s, even though the coarsening is not remarkable. These precipitates are fcc (Ti, Nb)(N, C) particles and belong to the MX-type precipitates. The beneficial effects of precipitation strengthening are lost. The hardness decreases to a minimum hardness value due to the presence of large amounts of polygonal ferrite after isothermal holding for 3600 s. Relatively coarse precipitates are the primary origin of the hardness decrease.

Keywords Microalloyed steel · Isothermal holding time · Microstructural constituent · Precipitation · Hardness

1 Introduction

High-strength low-alloy steels have been developed to substitute the low-carbon steels in space equipment and facilities, pressure vessels, offshore oil drilling platforms, building construction, storage tanks and the automotive industry to meet higher strength requirements [1–5]. These steels are relatively easy to be fabricated and have good strength and toughness with low carbon content [6, 7]. Moreover, the minor additions of alloying elements such as Nb, V, Ti and Mo enhance the mechanical properties via various mechanisms such as grain refinement, solid solution strengthening, precipitation hardening and increasing dislocation density [1–8].

Thermomechanical controlled processing (TMCP) consisting of controlled hot rolling followed by controlled cooling is used to maximize the benefits of the microalloy additions present in microalloyed steels [9]. Mechanical properties of steels depend on the phase constitutions of the final microstructures which can be related to the processing parameters [10]. The desired mechanical properties can be obtained through the optimization of alloy design and TMCP, which involve grain refinement in conjunction with microstructural control and precipitation strengthening [11, 12]. Precipitation hardening is one of the most common methods of increasing the strength and hardness of alloys [13, 14]. The precipitation behavior of the microalloyed steels has attracted lots of research interest [15]. The prevailing terms to describe the two distinguishable modes for alloy carbides formed at the γ/α interface have been "interphase precipitation carbides" and "fibrous carbides" [16]. The hardening effect of interphase precipitation has been shown to be more vital for the development of strong

✉ Qi Zhou
zhouqi2469@163.com

[1] School of Environment and Chemical Engineering, Shenyang Ligong University, Shenyang 110159, Liaoning, China

[2] College of Materials Science and Engineering, Shenyang Aerospace University, Shenyang 110136, Liaoning, China

[3] State Key Laboratory of Rolling and Automation, Northeastern University, Shenyang 110004, Liaoning, China

and tough hot-rolled steels with improved weldability due to the reduced carbon content [13–19]. However, microstructural features and precipitation in Ti, Nb and V microalloyed steel on isothermal holding have not been comprehensively studied. Thus, it is necessary to elucidate the phase and microstructure as well as the precipitation behavior of different isothermal conditions for this steel.

In this work, thermal simulations were conducted in the Ti, Nb and V microalloyed steel. The Vickers hardness distributions of the specimens were compared after different isothermal holding times. The microstructural features and the precipitation behavior were discussed after different isothermal holding times by the analysis of the microstructural constituents of the steel.

2 Experimental procedure

The composition of microalloyed steel studied in this work is given in Table 1. Cylindrical specimens were taken from hot-rolled material and machined in ϕ8 mm × 15 mm. Thermal simulation experiments were performed in a Gleeble 1500 thermomechanical simulator. The thermal simulation specimens were first heated to austenitic solution temperature (1200 °C) for 600 s, then deformed 33% (strain rate of 3 s^{-1}) at 1100 °C and 50% (strain rate of 10 s^{-1}) at 950 °C and followed by cooling to 600 °C and isothermal holding for 5, 10, 60, 600, 1800 and 3600 s, respectively. Finally, they were water quenched to room temperature in order to terminate further interphase precipitation (IP). The processing schedule of the thermal simulation experiment is shown in Fig. 1.

Six slabs (100 mm × 80 mm × 5 mm) were reheated to 1150 °C for 15 min, then cooled to 600 °C and isothermally held for 5, 10, 60, 600, 1800 and 3600 s in the electric resistance furnace and were finally water quenched to room temperature. Three specimens were cut from each piece of the slab. Tensile tests were carried out using an Instron 4206 machine to study the mechanical properties of the X90 linepipe steel. The product (R_m × A_{50}) of ultimate tensile strength (R_m) and total elongation (A_{50}) could be used to express the strength–ductility balance of the X90 linepipe steel. Measurements of the Vickers hardness used a total of five indentations under a load of 4.9 N for each specimen of the processing conditions. The specimens were etched with 4% Nital for optical microscopy (OM)

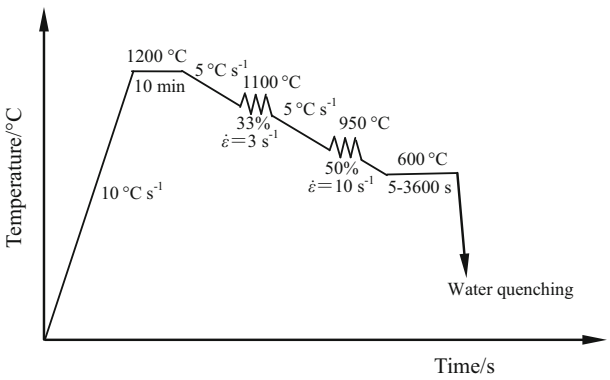

Fig. 1 Schematic illustrations describing thermal conditions of simulation. $\dot{\varepsilon}$ strain rate

observations. To highlight the microstructural constituent, the LePera method was used [20], after which this etched ferrite appeared gray, bainite appeared black and martensite and martensite–austenite (MA) islands appeared white. Optical microscopy observations were supplemented by scanning electron microscopy (SEM, SSX-550) and transmission electron microscopy (TEM, EM 400T). The foils for TEM were prepared by twin-jet polishing using a solution of 10% perchloric acid in methanol at temperature of − 30 °C and operating voltage of 40 V. The volume fractions of the precipitates were assessed with the IPP image analysis software.

3 Experimental results

3.1 Microstructural observations

The micrographs of the experimental steel after the simulations in different thermal conditions are shown in Fig. 2. Some martensites were observed when the specimen was isothermally held for 5 s at 600 °C (Fig. 2a), even though the characteristics of martensite observed in OM were not typical. Martensites and the transformed plates of bainitic ferrite could be seen in the specimens after isothermal holding for 5 s (Fig. 2g). Bainitic ferrite was the predominant structure of the microstructural constituent in the specimens for isothermal holding time of 5, 10, 60, 600, 1800 and 3600 s (Fig. 2a–f). Bainitic ferrite transformed at medium temperatures was lath-like, which is clearly shown in Fig. 2g–l. The polygonal ferrite formed after isothermal

Table 1 Chemical composition of experimental steel (wt.%)

C	Si	Mn	Al	S	P	Ti+Nb+V	Ni	Cr	Cu	Mo	N	Fe
0.059	0.23	1.87	0.025	0.0014	0.019	0.095	0.35	0.24	0.19	0.185	4.08×10^{-3}	Balance

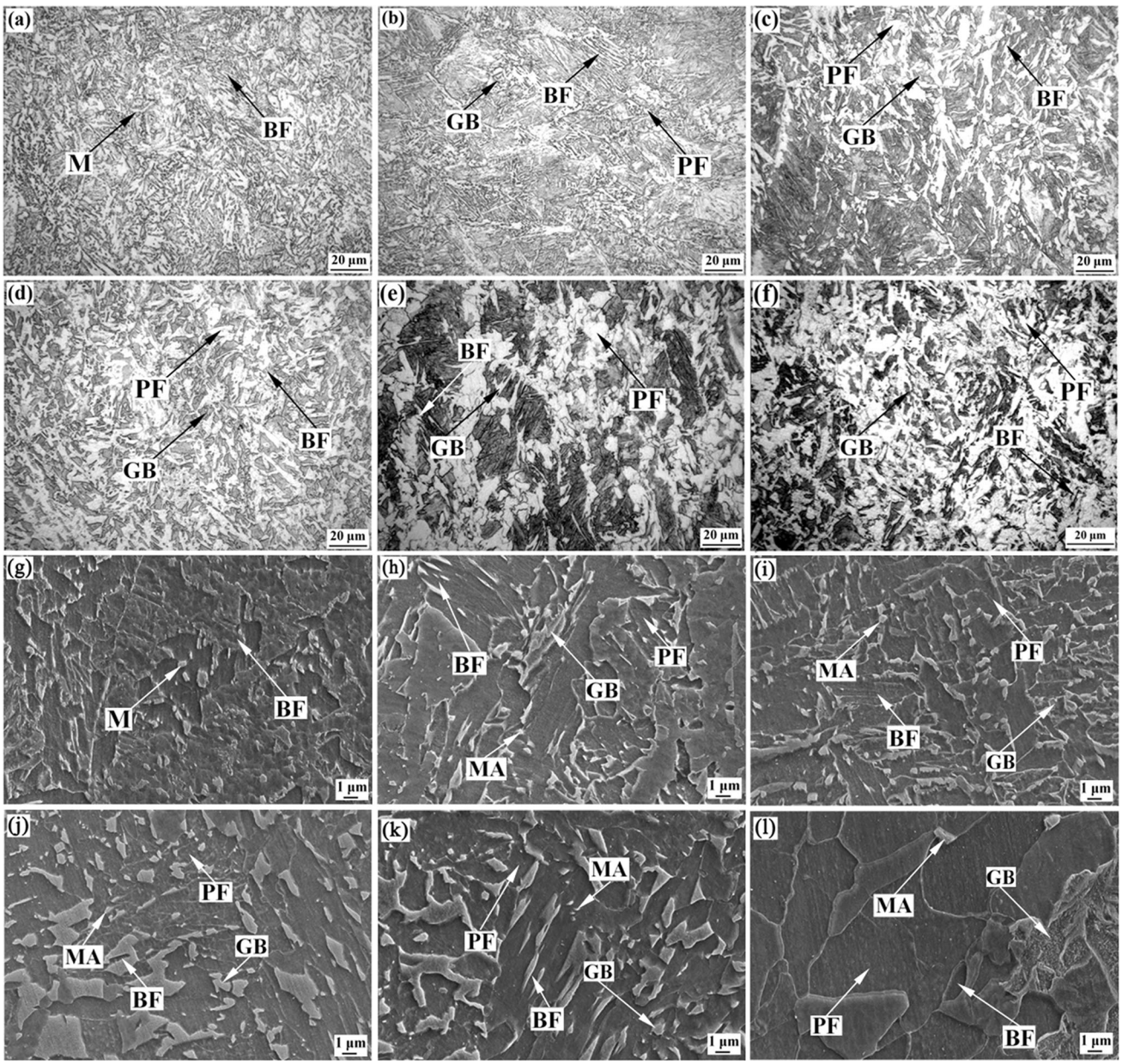

Fig. 2 OM and SEM micrographs of specimens held for 5 s (**a**, **g**), 10 s (**b**, **h**), 60 s (**c**, **i**), 600 s (**d**, **j**), 1800 s (**e**, **k**) and 3600 s (**f**, **l**). *M* martensite; *BF* bainitic ferrite; *GB* granular bainite; and *PF* polygonal ferrite

holding for 10, 60, 600, 1800 and 3600 s (Fig. 2b–f, h–l), and appeared white (Fig. 2a–f) and black (Fig. 2g–l) at OM and SEM, respectively. And it can be seen that fractions of granular bainite increased with increasing holding time for the specimens after isothermal holding for 10, 60, 600, 1800 and 3600 s (Fig. 2b–f, h–l).

The micrographs of the LePera specimens are shown in Fig. 3. The white martensite formed upon isothermal holding for 5 s had a massive appearance, and the remaining phases were the gray ferrite (Fig. 3a). The white MA islands were observed under different isothermal conditions, and particularly, they were fine and dispersed after isothermal holding for 600 s (Fig. 3d). The gray-colored ferrite formed after thermal simulation, and granular bainitic appeared black for the isothermal holding time of 1800 and 3600 s (Fig. 3e, f). The volume fractions of the microstructural constituents are given in Table 2. Maximum volume fraction (23.8%) of MA islands was obtained when the specimens were isothermally held for 600 s at 600 °C due to the increase in granular bainite amount.

Figure 4 shows TEM micrographs for the specimens after isothermal holding for 10, 600 and 3600 s, and it

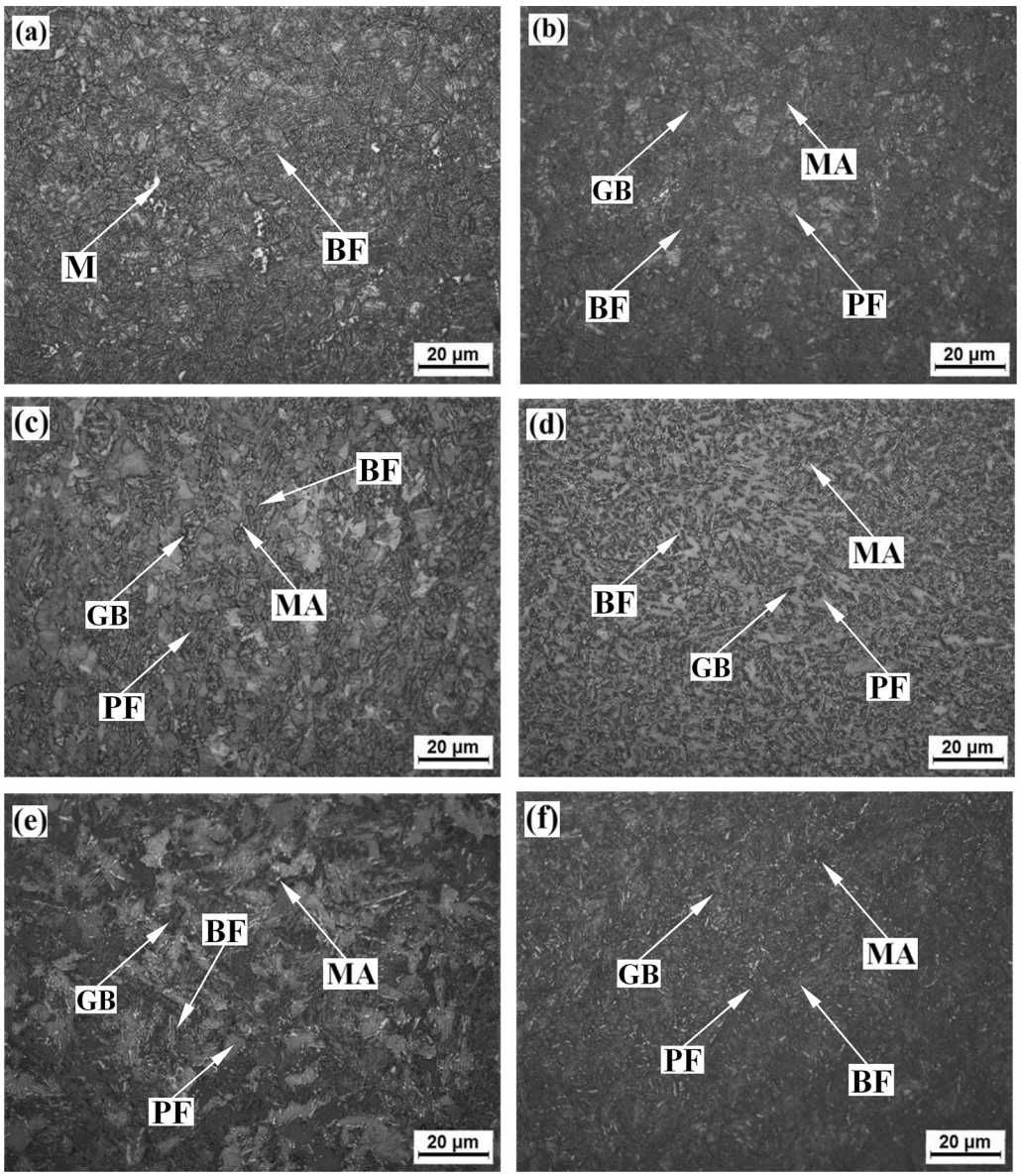

Fig. 3 Optical micrographs of experimental steel (etched by LePera) held for 5 s (**a**), 10 s (**b**), 60 s (**c**), 600 s (**d**), 1800 s (**e**) and 3600 s (**f**)

Table 2 Volume fractions of microstructural constituents

Isothermal holding time/s	Granular bainite/%	Bainitic (polygonal) ferrite/%	Martensite (martensite–austenite islands)/%
5	–	92.2 ± 3.1	7.8 ± 0.5
10	17.6 ± 3.8	79.2 ± 4.3	3.2 ± 0.3
60	23.6 ± 3.6	68.2 ± 0.6	8.2 ± 3.1
600	33.3 ± 4.1	42.9 ± 2.7	23.8 ± 0.5
1800	56.4 ± 4.4	37.4 ± 3.5	6.2 ± 2.1
3600	43.5 ± 5.2	46.1 ± 4.7	10.4 ± 2.2

indicates that all specimens show a bainitic structure. Polygonal ferrite can be observed in the specimen with isothermal holding for 10 s (Fig. 4a); as isothermal holding time increases to 600 s, the microstructure is mainly composed of MA islands and polygonal ferrite coexisted with bainitic ferrite (Fig. 4b); and as indicated in Fig. 4c, the existence of MA islands and bainitic ferrite in the specimen was associated with an isothermal holding time of 3600 s.

It was difficult to find any fine dispersed precipitates in the specimen after isothermal holding for 10 s. Undissolved Nb/Ti carbonitride precipitate was observed in the specimen, and its morphology was round shape. The diameter of these particles reached approximately 41 nm (Fig. 5a), and corresponding energy dispersive spectroscopy (EDS) analysis indicated that it was an undissolved Nb/Ti carbonitride precipitate (Fig. 5b).

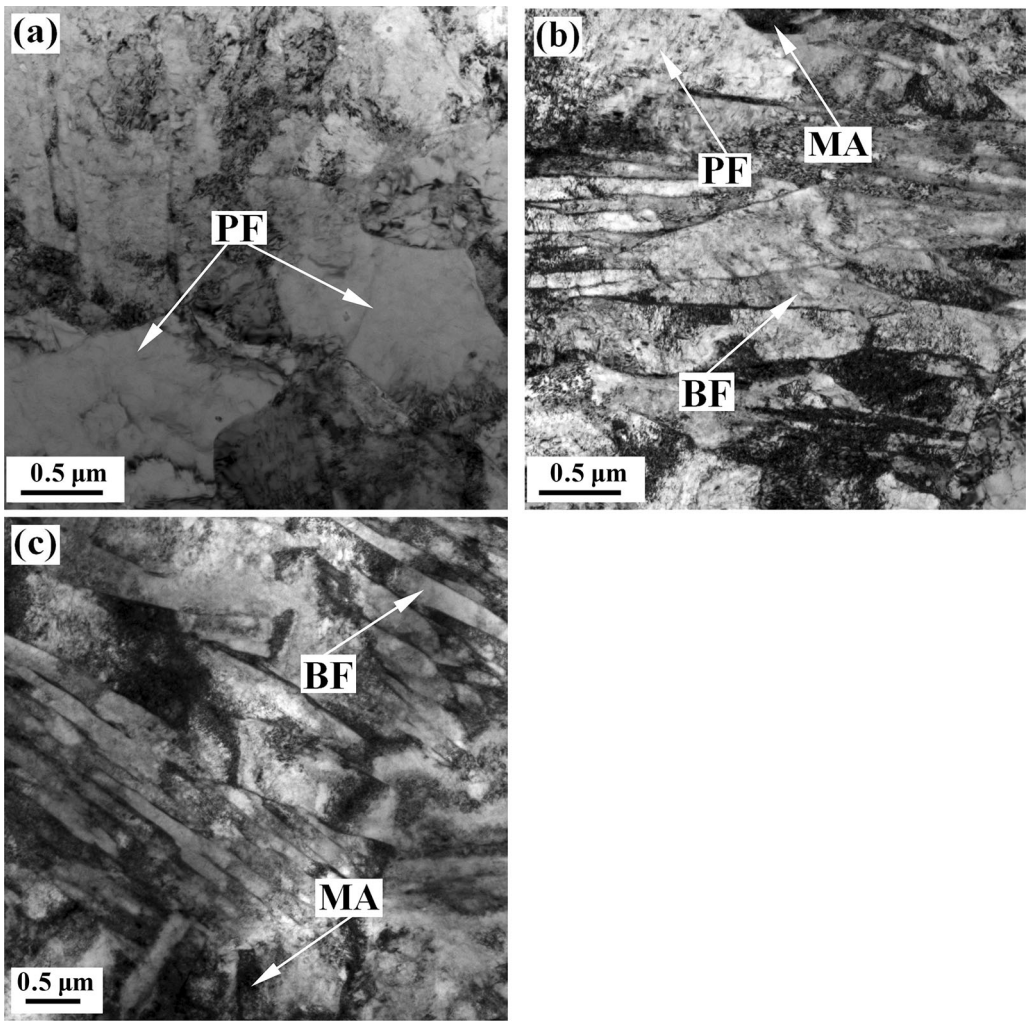

Fig. 4 TEM micrographs of specimens after isothermal holding for 10 s (**a**), 600 s (**b**) and 3600 s (**c**)

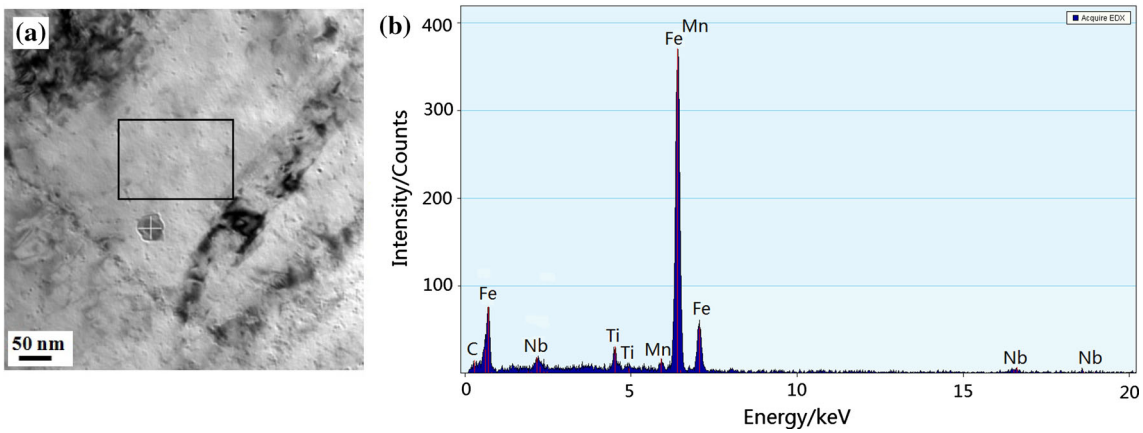

Fig. 5 TEM micrograph (**a**) and corresponding EDS result (**b**) of specimen after isothermal holding for 10 s

Fine dispersed precipitates were observed in the specimen after isothermal holding for 600 s (Fig. 6). These precipitates existed either in the grain boundaries or within the lattice structure of the bainitic ferrite. A selected area diffraction pattern (SADP) taken from a particle dispersed with a ferrite matrix (Fig. 6c) indicates that the particle was an fcc (Ti, Nb)(N, C) particle, which confirmed the presence of the MX-type precipitates.

Many precipitates adjacent to the grain boundaries formed in the specimen after isothermal holding for 3600 s (Fig. 7). The EDS analysis of the precipitate indicated that the larger particles were undissolved Nb/Ti carbonitride precipitates (Fig. 7a, b). An SADP taken from a particle shown in Fig. 7d, e indicates that the particle was fcc (Ti, Nb)(N, C) particles, which were also the MX-type precipitates. Precipitated particles coarsened with increasing holding time.

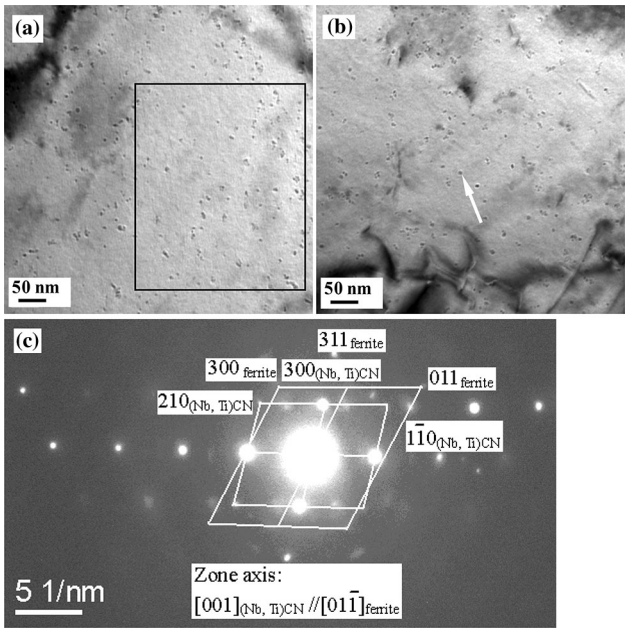

Fig. 6 TEM results of specimen after isothermal holding for 600 s. **a** Precipitated particle; **b** presence of a dark precipitate (denoted by an arrow) particle within the bainitic ferrite; **c** schematic illustration of SADP

The estimated volume fraction and average size of the precipitates are given in Table 3. The areas for measuring the volume fraction and average size of precipitates are indicated in Figs. 5a, 6a and 7c. The volume fraction of (Nb, Ti)CN is ignored because fine dispersed precipitates were insignificant when the specimen was isothermally held for 10 s at 600 °C, despite the presence of undissolved Nb/Ti carbonitride precipitate (average size of approximately 41 nm). The volume fraction of (Nb, Ti)CN precipitates rose abruptly with increasing holding time and reached its maximum fraction of 4.831% for the specimen after isothermal holding for 3600 s. The average size of the precipitates reached 4.226 nm when the specimen was isothermally held for 3600 s.

3.2 Mechanical properties

The average R_m, A_{50} and $R_m \times A_{50}$ of each group specimens are presented in Fig. 8. Mean square deviations of

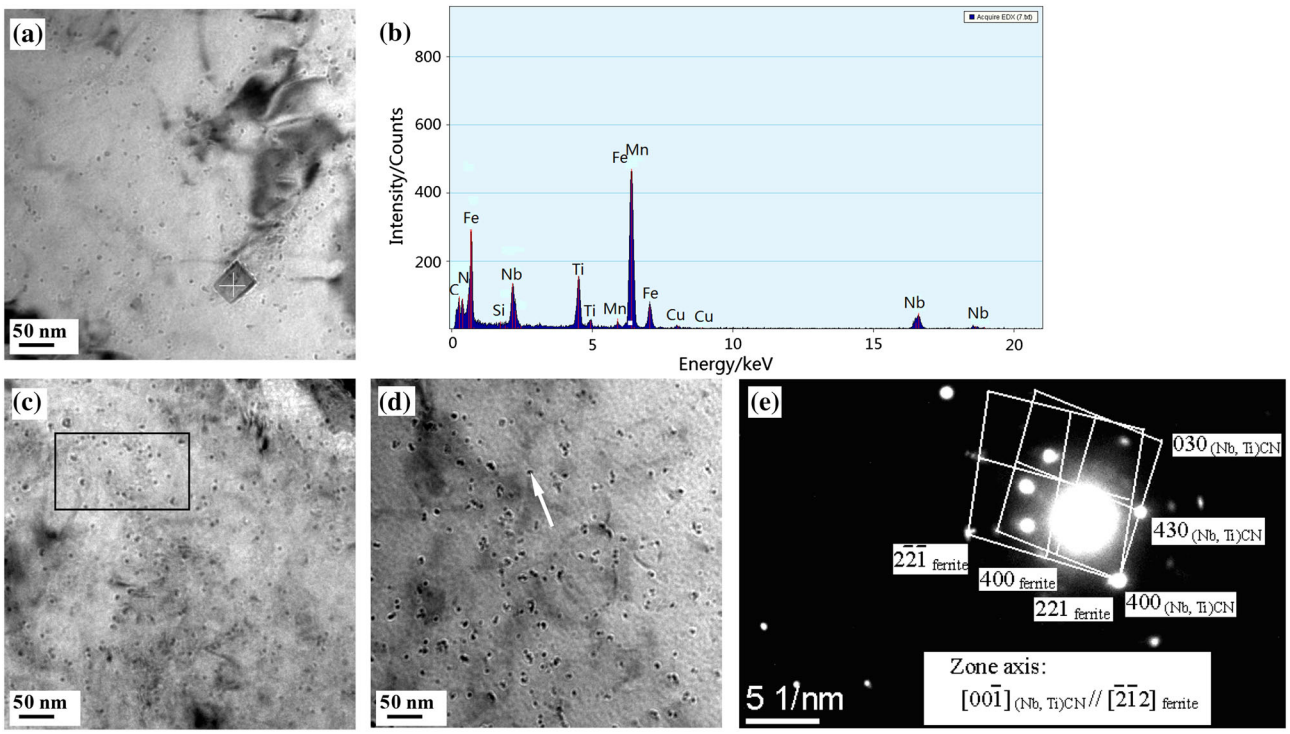

Fig. 7 TEM results of specimen after isothermal holding for 3600 s. **a** Precipitated particle; **b** corresponding EDS image of (**a**); **c** precipitate particle; **d** presence of a dark precipitate (denoted by an arrow) particle within the bainitic ferrite; **e** schematic illustration of SADP

Table 3 Measured volume fraction and average size of precipitates

Isothermal holding time/s	Volume fraction/%	Average size/nm
10	–	–
600	2.272	3.561
3600	4.831	4.226

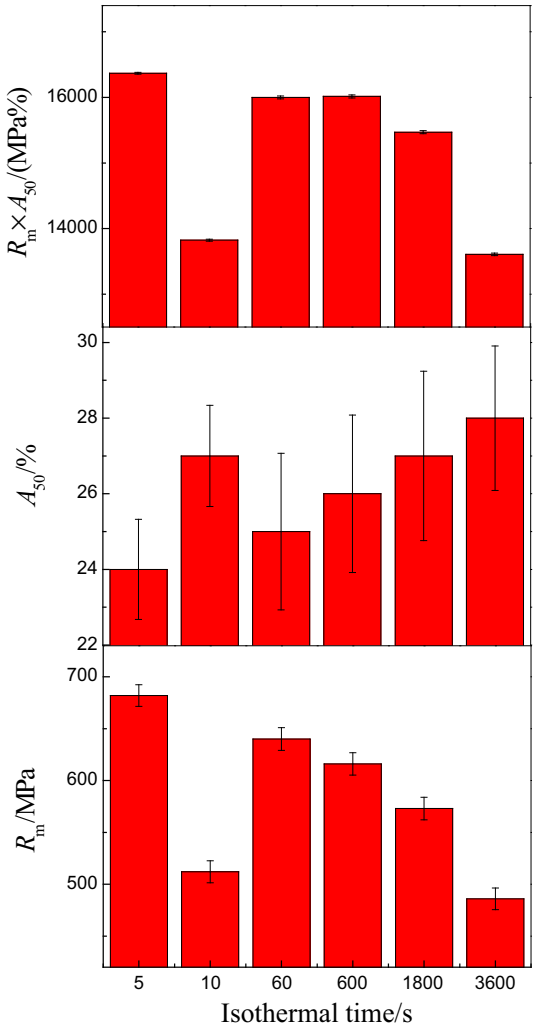

Fig. 8 Mechanical properties of specimen after different isothermal holding time

R_m, A_{50} and $R_m \times A_{50}$ were 69.12 MPa, 1.34% and 1093.19 MPa%, respectively. Figure 8 shows that the maximum R_m of 682 MPa was obtained after isothermal holding for 5 s due to the strengthening effect of martensite. The specimens exhibited very high R_m and $R_m \times A_{50}$ after isothermal holding for 60, 600 and 1800 s. This was due to the key role played by the precipitation strengthening. The specimen showed high R_m (640 MPa) after isothermal holding for 60 s. This was attributed to the precipitation strengthening of the fine dispersed precipitate particles. The lowest value of R_m (486 MPa) was obtained for the specimen after isothermal holding for 3600 s. This means that the precipitation strengthening was not notable. The $R_m \times A_{50}$ of the specimen reached the maximum value (16,368 MPa%) after isothermal holding for 5 s, because the martensite was formed after the evolution through the thermal condition of the simulations. This product reached the minimum value (13,608 MPa%) for the specimen after isothermal holding for 3600 s due to low value of R_m, which is related to the formation of large amounts of polygonal ferrite. On the other hand, the effects of precipitation strengthening were certainly lost.

3.3 Vickers hardness

The effect of the isothermal holding time on the hardness of the specimens at 600 °C for Ti, Nb and V microalloyed steel is shown in Fig. 9. Mean square deviation of the hardness value was 39.18 HV. The hardness of the specimens decreased overall with the increasing holding time at 600 °C. The maximum hardness of 287 HV was obtained after isothermal holding for 5 s due to the strengthening effect of the martensite. Then, the hardness decreased after isothermal holding for 10 s. This was due to the disappearance of the white martensite. The effect of the precipitation strengthening decreased solely due to the coarse, undissolved Nb/Ti carbonitride precipitate (Fig. 5b). Isothermal holding for 60 s resulted in an increase in the hardness (266 HV) due to the precipitation strengthening of the fine dispersed precipitate particles. Finally, the hardness decreased with the increasing holding time and reached the lowest value (174 HV), showing the same trend as the changes of mechanical properties.

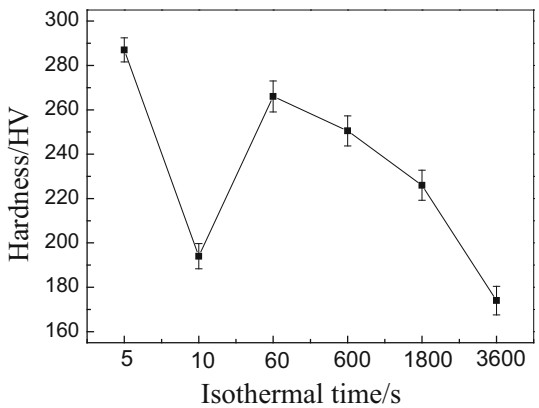

Fig. 9 Vickers hardness of specimens as a function of isothermal holding time at 600 °C

4 Discussion

The steel studied in this work, which contained the alloying elements such as Nb, Ti and V, was reheated at 1200 °C. The microalloyed carbonitride particles are firstly dissolved at 1200 °C and then precipitated by nucleation during the subsequent deformation, cooling and isothermal stages, thereby inhibiting recrystallization. Grain growth was sufficiently slowed down due to the pinning of the precipitates. Therefore, the final microstructure of the present steel after the thermal simulation experiment had the characteristic appearance of fine ferrite grains.

Microstructural evolution occurred after different isothermal transformation processes. There was a small quantity of martensites due to water quenching for specimens after the isothermal holding time of 5 s at 700 °C (Table 2). The dominant microstructural constituent of the steel was bainitic ferrite after isothermal holding for 10 s, and the effect of martensite (martensite–austenite islands) strengthening was limited due to a small quantity of the strengthening phase. Granular bainites began to form at this thermal simulation condition. The microstructure consisted of granular bainite and bainitic and polygonal ferrite for isothermal holding time of 10–3600 s. It consisted primarily of large amounts of polygonal ferrite after isothermal holding for 1800 s and 3600 s (Figs. 2 and 3).

Microstructural constituents are important factors for the enhancement of mechanical properties of the steel. The martensite strengthening effect is the most important origin of the improved mechanical properties according to the variational results for the Vickers hardness of the specimens, and the maximum hardness of 287 HV was obtained after isothermal holding for 5 s. Martensite disappeared from the specimen after isothermal holding for 10 s. The hardness value was relatively lower with martensite–austenite islands content of up to approximately 23.8% after isothermal holding for 600 s (Table 2). Granular bainite which contains equiaxed, island-shaped martensite–austenite constituents had a strengthening effect with prolonged holding. The boundaries between the GB laths are usually low-angle grain boundaries with small misorientation angles [21]. Therefore, it is difficult to observe these lath boundaries and only the packet boundaries can be revealed clearly [22]. The strengthening effect of granular bainite was the lowest for the specimen after isothermal holding for 10 s. The lath-like bainitic ferrite appeared, and the bainitic ferrite plate and granular bainite were the dominant microstructural constituents of specimens after isothermal holding for 10, 60, 600, 1800 and 3600 s (Table 2). The decrease in hardness was related to the presence of large amounts of polygonal ferrite after isothermal holding for 1800 and 3600 s (Fig. 9).

The ferrite grain size was fine due to the effect of the microalloying elements. A decrease in the grain size generally leads to an increase in the hardness [23]. However, the influence of the grain size on the hardness was insignificant in the present study, and the microstructural constituents and the precipitation strengthening had the decisive influence.

In the thermal simulation process, the microalloyed carbonitride particles provided effective precipitation strengthening, and in particular, the short isothermal holding time prevented the occurrence of any appreciable particle coarsening. However, it was difficult to find any fine dispersed precipitates because precipitation was rare in the specimen after isothermal holding for 10 s. Only some undissolved Nb/Ti carbonitride precipitates were observed during the deformation and the subsequent cooling and isothermal stages after the deformation under these thermal simulation conditions (Fig. 5). Vickers hardness of the specimens reached the maximum value due to the martensite strengthening effect for the specimen after isothermal holding for 5 s. Then, the hardness decreased after isothermal holding for 10 s because of the disappearance of the martensite. The effects of the precipitation strengthening did not give rise to a distinct advantage in this case.

According to Nafisi et al. [24], the strengthening contribution is calculated using the Ashby–Orowan model which adequately describes the strengthening of the precipitates with size of 3–30 nm and is given by:

$$\sigma = \alpha \frac{Gb}{2\pi L} \ln \beta \frac{r}{b} \tag{1}$$

where σ is the strengthening contribution; α and β are constants with values of 2.4 and 0.8, respectively; G denotes the shear modulus, which equals to 80.3 GPa; b is the magnitude of the Burgers vector which is 2.5×10^{-10} m; r is the particle radius; and L is the interparticle spacing given by $L = r\sqrt{2\pi/3f}$ (where f is the volume fraction of the precipitates). As described above, the undissolved Nb/Ti carbonitride precipitate, and carbonitride that precipitated during the high-temperature deformation and subsequent cooling and isothermal holding after dissolution, was observed. Fine dispersed precipitates were nearly absent in the specimen after isothermal holding for 10 s. Therefore, the strengthening contribution of the precipitates were infinitesimal because the volume fraction (f) was nearly zero (Table 3). This is the principal reason for the decrease in the hardness after the isothermal holding for 10 s.

As mentioned above, the hardening effect of the interphase precipitation is more vital for the present steel. Interphase precipitation can occur in ferrite at the austenite/ferrite interface, conferring significant coherency strengthening [25]. It is a major microstructural contributor to the hardness (strength). Interphase precipitation did not

occur, and therefore, the hardness of the specimen decreased after isothermal holding for 10 s.

The hardness increased and maintained a high value for the specimen after isothermal holding for 60 and 600 s, which was attributed to the contribution of the interphase precipitation hardening to the hardness of the studied steel. The interphase precipitation should have already begun for the specimen after isothermal holding for 60 s. Fine dispersed precipitates were clearly distinct for the specimen after isothermal holding for 600 s. They were fcc (Ti, Nb)(N, C) particles, which are MX-type precipitates (Fig. 6). The nanoprecipitates were formed through the transition of solute clusters and/or metastable precipitates with a composition and structure that was different from the stoichiometric equilibrium phase [26]. The hardness values of the specimens increased with increasing quantity of the dispersed carbonitride precipitates.

The variation in the hardness was also affected by the microstructural constituents. The results for the formation of large amounts of polygonal ferrite led to the decrease in the hardness for the specimen after isothermal holding for 1800 and 3600 s. On the other hand, the precipitates could grow into the matrix from the nuclei near the grain boundaries with prolonged holding. Many precipitate particles were observed in the specimen after isothermal holding for 3600 s. With the exception of the formation of the undissolved precipitates, these precipitated particles were also the MX-type precipitates (Fig. 7). It is worth noting that the present steel contained Mo, and the existence of Mo-rich precipitates was possible. Mo can reduce the size of the carbide precipitates and retard their coarsening behavior, because it enhances the nucleation rate by reducing the interfacial energy [27]. Therefore, the precipitates were coarse for the specimen after isothermal holding for 3600 s, and at the same time, the coarsening of the precipitates was not remarkable because the isothermal holding time was not sufficiently long. However, the beneficial effects of precipitation strengthening were still lost as the precipitates grew larger in size and spacing. The presence of large amounts of polygonal ferrite resulted in the decreased hardness after isothermal holding for 3600 s. On the other hand, relatively coarse precipitates were the primary reason for the decrease in the hardness.

We note that the low hardness was observed after isothermal holding for 10 s and was larger than that for the isothermal holding for 3600 s. It is suggested that the precipitation reaction should occur approximately when the specimen is isothermally held for 10 s, even though it is difficult to observe the precipitates (Fig. 5). The strengthening contribution of fine dispersed precipitates (except for the undissolved precipitates) was still present after isothermal holding for 10 s. This is the reason for the changes in the hardness values.

5 Conclusions

1. Martensite forms upon isothermal holding for 5 s. The bainitic ferrites are the predominant structure of the microstructural constituent of the specimens for 5, 10, 60 and 600 s. Granular bainite forms after isothermal holding for 10, 60, 600, 1800 and 3600 s. Ferrite exhibits a polygonal appearance with increasing holding time.
2. The maximum hardness is obtained for the specimen after isothermal holding for 5 s due to the martensite strengthening effect. The hardness of the specimen decreases after isothermal holding for 10 s, because the strengthening contribution of the fine dispersed precipitates decreases. The hardness of the specimen increases and maintains high values after isothermal holding for 60 and 600 s. This is attributed to the contribution of the interphase precipitation hardening to the hardness of the investigated steel.
3. The precipitates of the specimen are coarse after isothermal holding for 3600 s, even though the coarsening is not remarkable because the isothermal holding time is not sufficiently long. These precipitates are fcc (Ti, Nb)(N, C) particles, which are MX-type precipitates. The beneficial effects of precipitation strengthening are lost. A minimum hardness value is related to the presence of large amounts of polygonal ferrite after isothermal holding for 3600 s. Relatively coarse precipitates are the primary reason for the decrease in the hardness.

Acknowledgements This work was supported by the National High Technology Research and Development Program ("863" Program) of China (2015AA03A501) and the Liaoning Provincial Science and Technology Plan Project (2015020189).

References

[1] M. Masoumi, C.C. Silva, I.A. Lemos, L.F.G. Herculano, H.F.G. de Abreu, J. Mater. Eng. Perform. 26 (2017) 1531–1539.
[2] H. Guo, P. Zhou, A.M. Zhao, C. Zhi, R. Ding, J.X. Wang, J. Iron Steel Res. Int. 24 (2017) 290–295.
[3] C.C. Wang, C. Zhang, Z.G. Yang, J. Iron Steel Res. Int. 24 (2017) 177–183.
[4] J. Gou, Z.J. Liu, H. Jia, J. Iron Steel Res. Int. 25 (2018) 243–251.
[5] H. Li, F. Chai, C.F. Yang, C. Li, X.B. Luo, J. Iron Steel Res. Int. 25 (2018) 120–130.
[6] P. Gong, E.J. Palmiere, W.M. Rainforth, Mater. Charact. 124 (2017) 83–89.
[7] C. Dong, A.M. Zhao, X.T. Wang, Q.H. Pang, H.B. Wu, J. Iron Steel Res. Int. 25 (2018) 228–234.
[8] A. Karmakar, S. Biswas, S. Mukherjee, Mater. Sci. Eng. A 690 (2017) 158–169.
[9] P. Gong, E.J. Palmiere, W.M. Rainforth, Acta Mater. 119 (2016) 43–54.

[10] H. Zhao, B.P. Wynne, E.J. Palmiere, Mater. Charact. 123 (2017) 339–348.
[11] S. Liu, V.S.A. Challa, V.V. Natarajan, R.D.K. Misra, D.M. Sidorenko, M.D. Mulholland, M. Manohar, J.E. Hartmann, Mater. Sci. Eng. A 683 (2017) 70–82.
[12] L. Sanz, B. Pereda, B. López, Mater. Sci. Eng. A 685 (2017) 377–390.
[13] M.F. Francis, W.A. Curtin, Acta Mater. 106 (2016) 117–128.
[14] S.Q. Bao, Y. Xu, G. Zhao, X.B. Huang, H. Xiao, C.L. Ye, N.N. Song, Q.M. Chang, J. Iron Steel Res. Int. 24 (2017) 91–96.
[15] J.G. Jung, J.S. Park, J. Kim, Y.K. Lee, Mater. Sci. Eng. A 528 (2011) 5529–5535.
[16] H.W. Yen, P.Y. Chen, C.Y. Huang, J.R. Yang, Acta Mater. 59 (2011) 6264–6274.
[17] S. Clark, V. Janik, Y. Lan, S. Sridhar, ISIJ Int. 57 (2017) 524–532.
[18] G. Miyamoto, R. Hori, B. Poorganji, T. Furuhara, ISIJ Int. 51 (2011) 1733–1739.
[19] S.F. Medina, L. Rancel, M. Gómez, R. Ishak, M. De Sanctis, ISIJ Int. 48 (2008) 1603–1608.
[20] E. Girault, P. Jacques, P. Harlet, K. Mols, J. Van Humbeeck, E. Aernoudt, F. Delannay, Mater. Charact. 40 (1998) 111–118.
[21] A. Lambert-Perlade, A.F. Gourgues, A. Pineau, Acta Mater. 52 (2004) 2337–2348.
[22] K. Zhu, D. Barbier, T. Lung, J. Mater. Sci. 48 (2013) 413–423.
[23] J.T. Zhang, Y.G. Zhao, J. Tan, X.X. Feng, J. Iron Steel Res. Int. 22 (2015) 157–162.
[24] S. Nafisi, B.S. Amirkhiz, F. Fazeli, M. Arafin, R. Glodowski, L. Collins, ISIJ Int. 56 (2016) 154–160.
[25] D.P. Dunne, Mater. Sci. Technol. 26 (2010) 410–420.
[26] I. Timokhina, M.K. Miller, J.T. Wang, H. Beladi, P. Cizek, P.D. Hodgson, Mater. Des. 111 (2016) 222–229.
[27] J.H. Jang, Y.U. Heo, C.H. Lee, H.K.D.H. Bhadeshia, W.S. Dong, Mater. Sci. Technol. 29 (2013) 309–313.